Grafting Hole-Transport Precursor Polymer Brushes on ITO Electrodes: Surface-Initiated Polymerization and Conjugated Polymer Network Formation of PVK

Timothy M. Fulghum, Prasad Taranekar, and Rigoberto C. Advincula*

Department of Chemistry and Department of Chemical and Biomolecular Engineering, University of Houston, Houston, Texas 77204

Received February 15, 2008; Revised Manuscript Received June 3, 2008

ABSTRACT: We have utilized surface-initiated polymerization (SIP) to functionalize the conducting transparent electrode, indium tin oxide (ITO) with polyvinylcarbazole (PVK) brushes. Atomic force microscopy (AFM) imaging revealed smooth domains of grafted PVK and the composition, confirmed by X-ray photoelectron spectroscopy (XPS) measurements. The PVK is an electrochemically cross-linkable precursor by virtue of the pendant carbazole group and thus capable of forming conjugated polymer network (CPN) films. The electrochemical behavior and oligocarbazole CPN formation were evaluated by cyclic voltammetry (CV) measurements. The covalent linkage of the PVK brush allowed for a direct electroluminescent device preparation on SIP modified ITO in which PVK acts as a hole-transporting layer. In this case, the polyfluorene copolymer can be easily spin-casted on top of the grafted PVK without dissolution problems. This resulted in an improved polymer light-emitting diode (PLED) device behavior where the EL polymer layer can be simply solution cast on the modified ITO irrespective of solubility.

Introduction

The use of π-conjugated organic polymer materials has shown great promise for the fabrication of organic and hybrid optoelectronic devices.[1] They have been utilized as active electroluminescent, photoconducting, electron-transporting, hole-transporting, and ion-dopable polymer materials. Other types of organic polymers have been used as ancillary materials to support the high performance of conjugated polymers in actual devices. One of the most widely utilized of these materials is poly(*N*-vinylcarbazole) (PVK).[2] It exhibits interesting electrooptical and charge-carrier properties in light-emitting diode devices,[3] solar cells,[4] nonvolatile memory,[5] and electrochromic devices.[6,7] Specifically for organic semiconductor and display devices, PVK shows good hole-transport properties, which is important for improving the performance of organic electroluminescent devices from the anode side.[8–13] Others have reported their application in amperometric chemical sensors, which allow controlled selectivity and sensitivity due to variable electron transport properties of doped and dedoped carbazole.[14,15] PVK exhibits these interesting properties primarily due to the carbazole group. On the other hand, an *all* 3,6-position linking of the carbazole units will lead to the formation of conjugated oligomeric to polycarbazoles units.[16–18] The synthesis of polycarbazoles is also of great interest for electrical conductivity and electrochromic device applications. Several groups have investigated its electropolymerization on Pt and Au substrates.[19,20]

Recently, the conversion of "precursor polymers" to form conjugated polymer network (CPN) films on conducting surfaces has been reported.[21–27] The approach consists of synthesizing a precursor polymer, which by design contains pendant electroactive monomer units. Electropolymerization or chemical oxidation results in a CPN film having both inter- and intramolecular cross-linkages between the pendant monomer units. The films formed are characterized by high optical quality (transparency), uniform coverage, good adhesion, smoothness in morphology, and controlled ion permeability.[28] Moreover, by controlling the amount of conjugated species and doping, it should be possible to control electrical conductivity.[29] Thus, the process is interesting for depositing *insoluble* cross-linked ultrathin films of conjugated polymers for practical electrooptical applications. A variety of combinations should be possible for the design of a precursor polymer backbone and the "electroactive monomer" side group to form the CPN film. It is also possible to *copolymerize* with small molecule electroactive monomers with varying compositions in order to control the degree of cross-linking and linear polymer formation. We have used these materials to a number of possible applications toward electroluminescent devices.[30,31] There has also been recent work focused on nanopatterning of precursor polymers, including PVK and several others, for possible applications in static[32,33] memory devices.

Surface-initiated polymerization (SIP) has the advantage in that surface properties can be easily modified by varying the composition of the polymer brush, grafting density, and the degree of polymerization or MW.[34] In general, there are two distinct pathways to achieve a polymer brush architecture, the first being the "grafting to" approach and the second being the "grafting from" approach. The "grafting to" approach generally utilizes amphiphilic or block polymers with an end functionality that interacts or anchors with the substrate surface. This generally involves a chemical or physical adsorption process. Limitations to this type of application are that the process is diffusion limited so that as more and more polymer chains are attached to the surface, the ability for a new polymer chain to diffuse to the surface of the substrate is greatly hindered. On the other hand, the "grafting from" or SIP approach holds the benefit of placing the initiating groups directly on the surface, allowing synthetic control of the polymer formation and grafting density. Locating the initiator on the surface means that the growing polymer is attached to the surface and the monomer diffuses to the growing chain end throughout the reaction; i.e., the growing chain eventually extends from the substrate. The technique is amenable to a number of surface initiators as well as various mechanisms of polymerizations.[35] Recently, Carter et al. have successfully reported the grafting of disubstituted

* To whom correspondence should be addressed. E-mail: radvincula@uh.edu.

10.1021/ma800341a CCC: $40.75
Published on Web 07/15/2008

Scheme 1. Synthesis Scheme for the Monochlorosilane AIBN Derivative, (*E*)-2-(Chlorodimethylsilyl)ethyl-4-((5-butoxy-2-cyano-5-oxopentan-2-yl)diazenyl)-4-cyanopentanoate (AIBNSiCl)

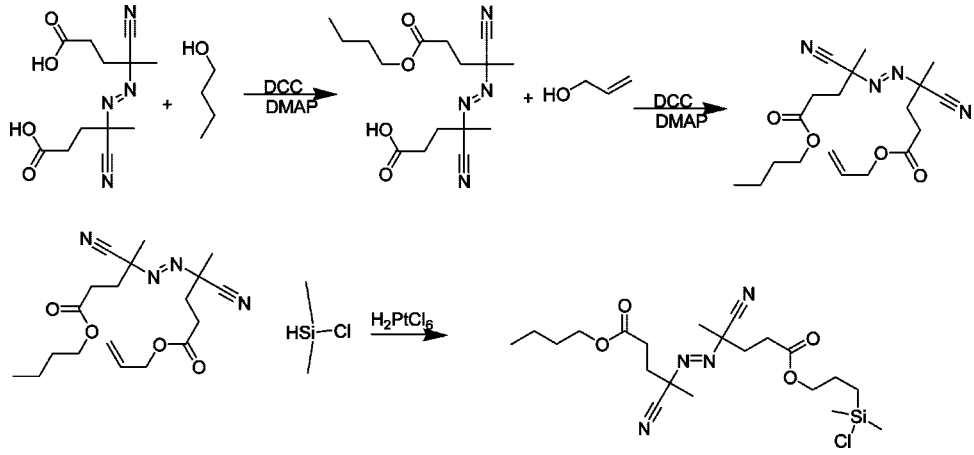

Scheme 2. Surface Functionalization of Hydroxylated Substrate with AIBNSiCl and Subsequent SIP of PVK; Summary of Polymerization Results Is Also Included

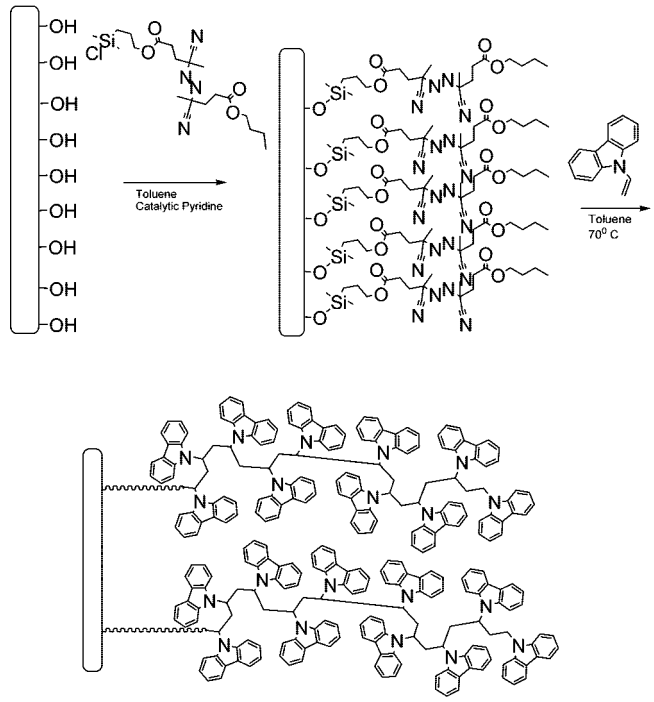

polyacetylene brushes grown from modified silicon and quartz surfaces using a transition-metal-catalyzed polymerization technique.[36]

The conventional method for preparing hole-transport polymer layer films involve solution-casting and spin-casting.[37,38] The problem with this method is that the electroluminescent active polymer layer is also spin-cast on top of the hole-transport layer, resulting in dissolution of the former film. Recently, the groups of Huck and Friend have demonstrated the use of SIP to produce tethered polyacrylates, containing triarylamine pendant groups as hole transport materials, for use in photovoltaic devices.[39,40] The devices exhibited enhanced charge carrying function as compared to devices prepared from solution-casting methods. This was attributed to controlled polymer architecture and morphology resulting in better charge-carrier transport properties for the device.

In this work, our goal is to utilize SIP to functionalize conducting transparent substrates like indium tin oxide (ITO) with PVK brushes. We have demonstrated the growth of PVK brushes directly from ITO, allowing for controlled grafting density and brush length. Moreover, inhomogeneities on the morphology of the ITO can be passivated. The PVK is electrochemically cross-linkable by virtue of the precursor architecture of the pendant carbazole group, capable of forming CPN films of oligo- and polycarbazole units. However, the main advantage is that an electroluminescent polymer, e.g. polyfluorene, can be easily spin-casted on top of the grafted PVK. Note that in most PLED device fabrication procedures dissolution of the polymer hole injecting layer during spin-coating of the electroluminescent layer is a problem, especially if their solubilities are similar. However, the grafting of PVK allowed for a direct device preparation on the SIP-modified ITO without solubility problems. This resulted in a viable polymer light-emitting diode (PLED) device fabrication protocol where, in principle, other EL polymer layers can simply be solution-cast irrespective of their solubility. We have also previously reported the preparation of carbazole methacrylate polymer thin films

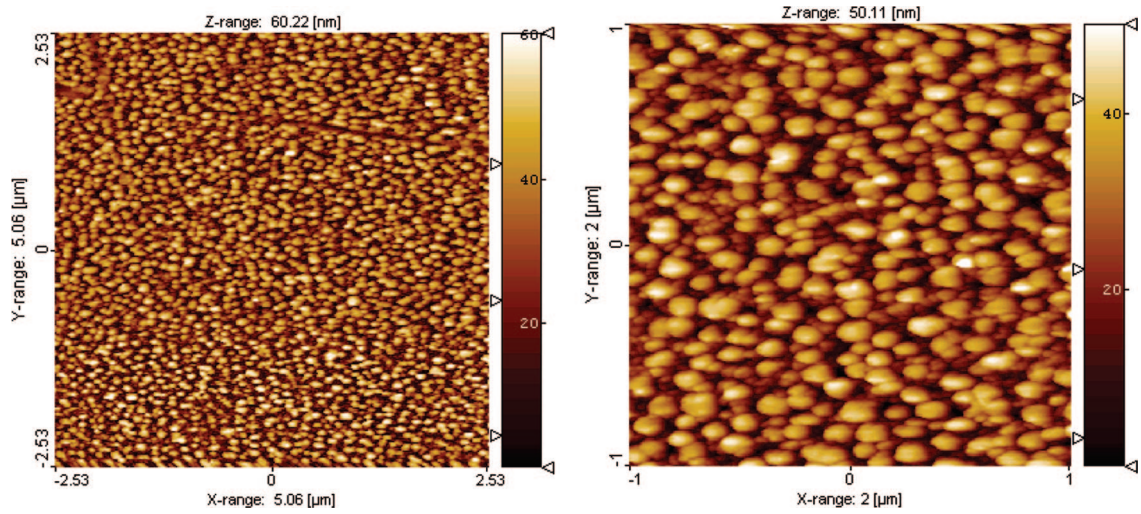

Figure 1. PVK brush topographical AFM images taken with MAC noncontact mode imaging. Left image is a 5 × 5 μm survey scan with high surface coverage and an rms roughness of 5.35 nm, as calculated with SPIP software. The right image is a 2 × 2 μm scan with an rms value of 4.91, showing an average grain size of ca. 150 nm in diameter.

chemically bound to a substrate surface by physical vapor deposition (PVD) and have evaluated their PLED behavior.[40,48]

Results and Discussion

Substrate Modification. The surface bound free radical initiator, (*E*)-2-(chlorodimethylsilyl)ethyl 4-((5-butoxy-2-cyano-5-oxopentan-2-yl)diazenyl)-4-cyanopentanoate (AIBNSiCl) (Scheme 1), was successfully synthesized and used for substrate modification. The procedure and characterization are described in the Experimental Section and is very similar to that reported by Rühe et al.[41,43] Decomposition studies with thermogravimetric analysis (TGA) of the initiator showed an initial decomposition temperature at 120 °C with 6.34% weight loss corresponding to the activation and evolution of N_2 gas from the material (see Supporting Information). This decomposition temperature and composition are the same as those for the monochlorosilane AIBN derivative reported by Rühe et al. and for unbound AIBN.[41] The initiators were then grafted onto a Si wafer and ITO substrate using the substrate modification procedure outlined in the Experimental Section. Ellipsometric data on Si-modified substrate showed a layer thickness of 1.5 nm; this value is less than the 2.1 nm length of the molecule (MM2 energy minimization calculations carried out with Chem3D, CambridgeSoft Corp.) but comparable to that reported by Ruehe et al.[43a] The variation in the thickness may be due to a less homogeneous monolayer formation, inherent tilt angle of the self-assembled monolayers (SAMs), or a combination of the two. AFM analysis of the initiator-coated samples showed a uniform coating with a root-mean-square (rms) roughness of 0.6 nm for the Si wafer. The morphology is also shown for the ITO-modified substrate, indicating much greater surface roughness (see Supporting Information).

Surface-initiated polymerization was carried out at 70 °C for periods ranging from 6 to 24 h (Scheme 2). After removal of the Schlenk flask from the temperature-controlled oil bath, it was allowed to cool to room temperature under ambient conditions. The free polymer and solvent were decanted carefully into cold hexanes to precipitate nongrafted polymer. The substrates were then removed and placed in the Soxhlet extractor for further purification. The precipitated polymer was filtered and redissolved in THF and then added dropwise to cold hexanes to reprecipitate the polymer. The polymer was filtered and dried in a vacuum oven at 40 °C for 24 h prior to gel permeation chromatography (GPC) analysis. Free polymer was analyzed to give a rough estimate of the PDI and MW of the surface bound polymer.[42,43] The molecular weight (MW) and polydispersity (PDI) for a reaction time of 24 h were M_n = 10 400 g/mol and M_w/M_n = 2.6, respectively. Ellipsometric measurements on the PVK brushes on ITO showed thicknesses in the range of 30−45 and 15 nm on Si wafer (summary in Supporting Information). Microscopic surface analysis of the films was measured through the MAC mode, a noncontact mode of AFM. A 5 × 5 μm survey scan is seen in Figure 1, which showed excellent homogeneous surface coverage and an rms roughness value of 5.35 nm. Analysis of the 2 × 2 μm scan easily showed the grain size of the brush to be ca. 150 nm in diameter. In principle, these morphologies can be further improved by annealing or solvent treatment procedures as in the case of most grafted polymer brushes.[35] Nevertheless, these morphological features are in contrast to the rough ITO surface that was initially used for the SIP in which large domains and highly visible grain boundaries were observed (see Supporting Information). Also, the rms roughness is of the order of 15 nm (or higher in most cases) varying from substrate to substrate. While this may not represent a typical rms roughness from a variety of ITO sources, it indicates that surface passivation of ITO morphological defects can be achieved by the direct grafting of a polymer film.

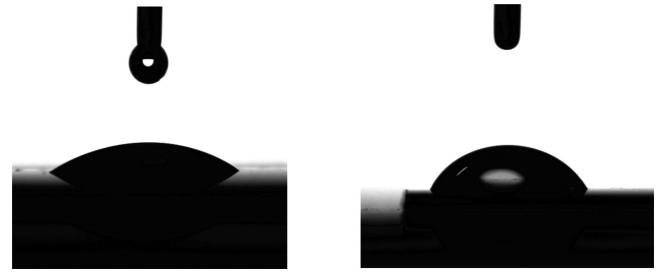

Figure 2. Static water contact angle (WCA) measurements on the (a) initial initiator-modified ITO substrate (30° in water) and to that of the (b) grafted PVK by SIP on ITO (55° in water).

Static water contact angle (WCA) measurements revealed a decrease in surface energy from the initial initiator-modified ITO substrate (30° in water) to that of the grafted PVK by SIP on ITO (55° in water), as shown in Figure 2. The WCA for well-cleaned ITO is below 10° and showed almost complete wetting in most cases. This indicates that the more hydrophobic PVK was successfully grafted onto the ITO surface, modifying the wetting behavior. Other values for the different polymerization times and substrates are summarized in the Supporting

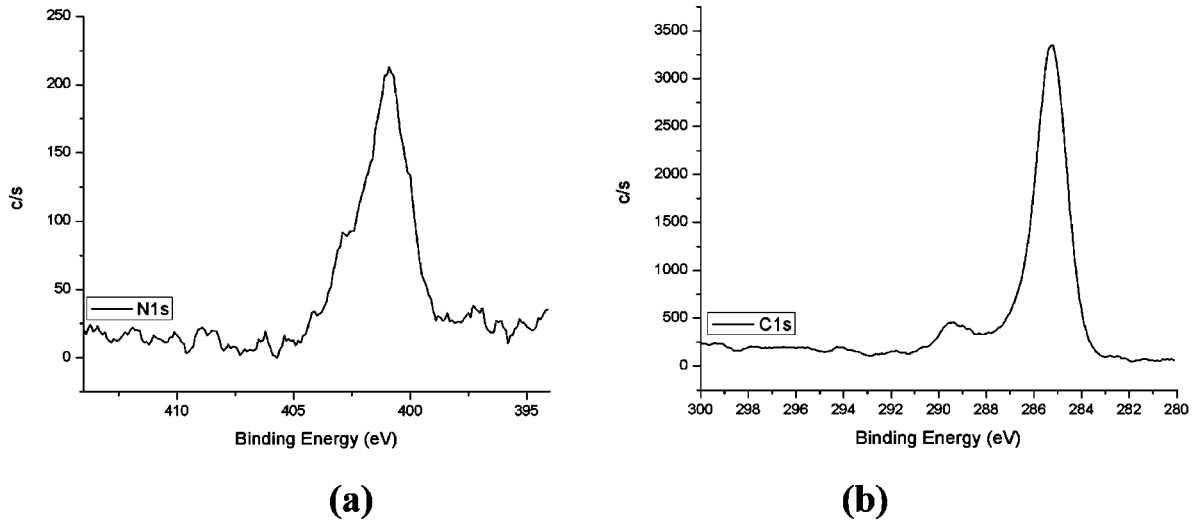

Figure 3. High-resolution XPS scans of the PVK brush on ITO substrate used for identifying the C and N composition ratios. The calculated ratio of carbon to nitrogen in the monomer, and thus the polymer, is 14:1, respectively, which coincided exactly with the ratio of carbon to nitrogen by XPS at 14:1 for PVK.

Information. In principle, it is possible to modify the wetting and swelling properties of such grafted brushes by solvent or temperature treatments as demonstrated by Zauscher et al. on grafted poly(*N*-ispropylacrylamide) brushes.[44]

XPS analysis was performed at a takeoff angle of 45° for elemental analysis and surface content ratio. High-resolution scans of the carbon (C) and nitrogen (N) regions were obtained and then fitted with Gaussian equations for peak area analysis (Figure 3). The calculated ratio of carbon to nitrogen in the monomer, and thus the grafted polymer, is 14:1, respectively, which coincided exactly with the ratio of carbon to nitrogen by XPS at 14:1 for PVK. For the initiator, previous studies of grafting onto a Si wafer showed the observed C/N atomic concentration ratio (84:16) correlates well with the grafted azo initiator composition, that is, 21 C atoms to 4 N atoms.[43b]

Electrochemistry. The PVK-modified ITO substrates were removed from the Soxhlet extractor and placed in a 0.1 M tetrabutylammonium hexafluorophosphate (TBAH) solution in CH_2Cl_2. This substrate served as the working electrode, and a Pt plate and Ag/AgCl reference electrode were utilized. The substrate was scanned at 20 mV/s from −50 to 1300 mV for up to 46 cycles in order to cross-link the PVK film forming the CPN cross-linked PCZ film (Figure 4). The onset of oxidation occurred at about 1.05 V in the first cycle, ∼150 mV higher than that observed from solution deposition of PVK.[29,45] The decrease in the onset of the oxidation peak is clear evidence of a lower oxidation potential for extended conjugated specie than the monomeric carbazole specie.[20,23,27,29,45] The current increases with increasing cycles indicating the electropolymerization of the carbazole units with each cycle. Compared to the electropolymerization of spin-coated films, the shift of the oxidation peak from the first cycle to the subsequent cycles was more gradual, possibly indicating the consequence of increase in polymer chain density with smoother and homogeneous film morphology. Scan rate dependence studies of the cross-linked PVK CPN at scan rates of 10−200 mV/s in a 0.1 M TBAH/CH_2Cl_2 electrolyte solution (potentials reported against the Ag/AgCl reference electrode) revealed a more surface-limited diffusion (nonlinear) behavior compared to what has been observed with CPN films from solution electropolymerized PVK (Figure 5).[23] This could indicate a slower electron transfer rate possibly due to the higher grafting density of the brush.

Examination of the films by UV−vis before and after the electropolymerization showed a large spectral difference arising from the formation of conjugated oligocarbazole species (Figure 6). Utilizing the lower energy threshold of the adsorption spectra of the polymer brush, the energy bandgap (E_g) was calculated to be 3.44 eV, which correlates well to the reported value of 3.5 eV.[12] Utilizing the same transition in the cross-linked polycarbazole film, a calculated E_g of 3.2 eV was observed, which also correlated to literature values.[46] The HOMO values were estimated to be 5.2 eV on the basis of band-gap determination protocol from the absorbance onset and CV measurements (see Supporting Information). Note that the HOMO level for PEDOT/PSS is 5.0 eV.[37] The clearly defined peaks at 342 and 352 nm visible in the PVK brush are eliminated; a tailing peak at 310 nm with a shoulder at 335 nm is attributed to the new $\pi \rightarrow \pi^*$ transition of a PCZ, and a polaronic band is observed centered at 424 nm.[45,47,48] These observations are consistent with our previous studies on electropolymerized PVK (CPN conversion to oligocarbazole) absorbance.[29,31] Lastly, AFM imaging revealed that electropolymerization and cross-linking resulted in a smooth homogeneous film characterized by the absence of regular domains as observed in the PVK brush (see Supporting Information).

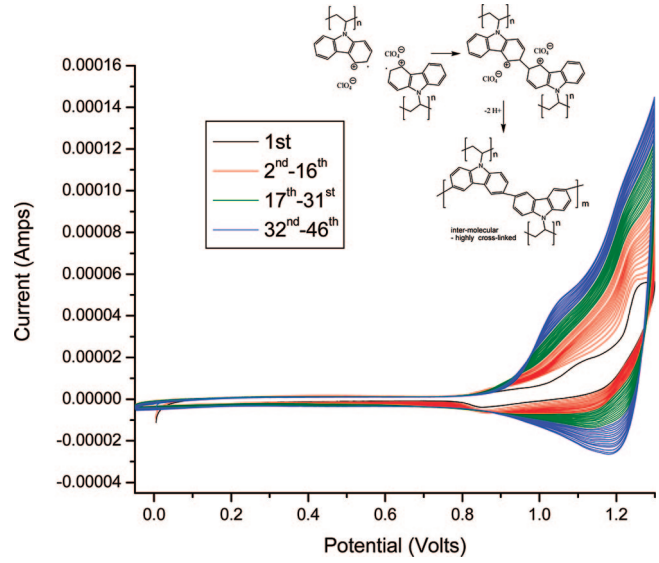

Figure 4. Cyclic voltammetry (46 cycles) of 45 nm PVK brush from −50 to 1300 mV at 20 mV/s. PVK-coated ITO as working electrode, Ag/AgCl as reference, and Pt plate as counter. Onset of oxidation for the first cycle is 1050 mV and subsequently decreases to 900 mV.

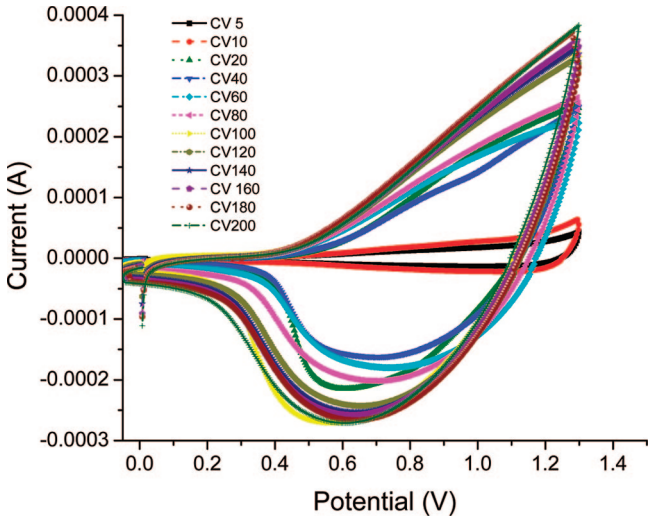

Figure 5. Scan rate dependency study of PVK brushes at scan rates of 10−200 mV/s in a 0.1 M TBAH/CH_2Cl_2 electrolyte solution. Potentials reported against the Ag/AgCl reference electrode.

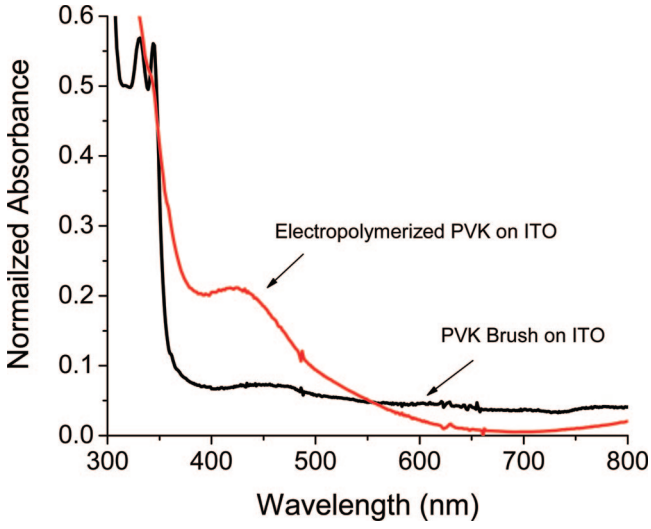

Figure 6. UV−vis absorption of PVK and electrochemically cross-linked PVK (EPVK). Absorption spectra of PVK are filled squares, and the EPVK is open circles.

PLED Studies. Double-layer PLED devices were assembled to investigate the current density (I_d)−voltage (V) characteristics of the polymers. The device structure consisted of the PVK SIP-modified ITO (45 nm), spin-coated poly(cyanofluorene-*alt*-*p*-phenylenevinylene) or PCNPV electroluminescent layer and evaporated Al layer for cathode. The PCNPV has been previously reported to have a LUMO of 3.07 and HOMO of 5.42 or a band gap of 2.35 V.[37] The forward bias current was obtained when the ITO electrode was positively biased and the aluminum was negatively biased. The device showed a relatively low turn-on voltage of 4.0 V in both the $I-V$ and $L-V$ measurements in air with current and luminance reaching 3000 mA/cm^2 (7.7 V) and 2000 Cd/m^2 (5.0 V) (Figure 7). For the 30.4 nm thick SIP brush, the turn-on voltage is at 6.5 V in both the $I-V$ and $L-V$ measurements in air with current and luminance reaching 1500 mA/cm^2 (7.5 V) and 2000 Cd/m^2 (6.0 V) (see Supporting Information). These values are much improved (lower turn-on voltage) over results from other systems utilizing PVK as the hole transport layer but with different EL materials[8,38] and comparable to the same EL material (PCPNV) with PEDOT/PSS as the hole-transport material with efficiencies of 1.96 lm/W (2.7 cd/A) at 5.0 V.[37] In this case, the PVK film (5.2 eV) is able to maintain a very good ohmic contact between the ITO

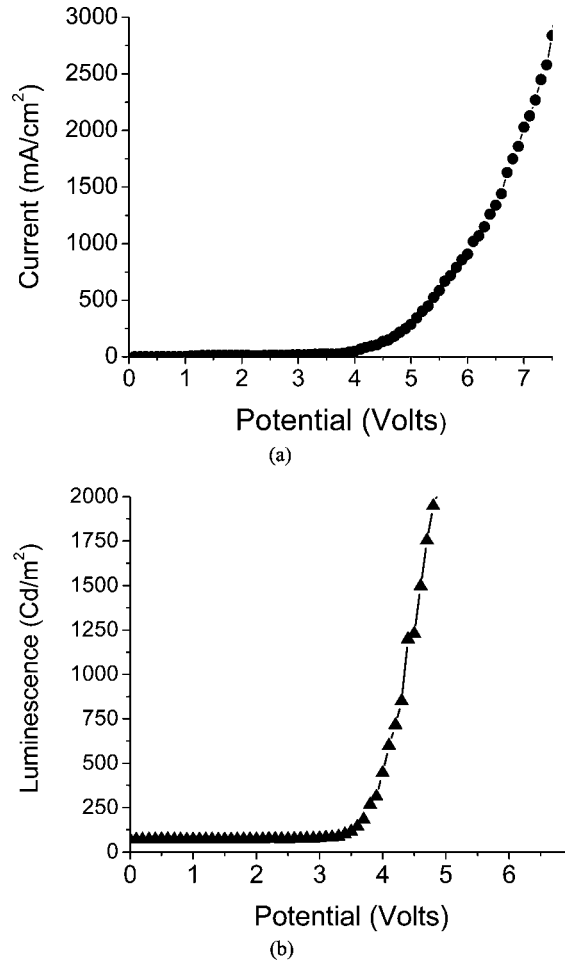

Figure 7. PLED analysis curves: (a) current (I) vs voltage (V) curve and luminescence (L) vs voltage (V). Current−voltage and luminescence−voltage data were collected from 0 to 10 V at steps of 0.10 V. Current is expressed in mA/cm^2 and luminance in Cd/m^2. These results are comparable to PCPNV with PEDOT/PSS as the hole-transport material with efficiencies of 1.96 lm/W (2.7 cd/A) at 5 V.[37]

(4.7 eV) and the PCNPV layer (5.4 eV) based on a proper match of the HOMO−LUMO levels and the ITO work function (see Supporting Information). A recent publication in collaboration with the Usui group on OLED devices prepared from surface-initiated poly(3-(*N*-carbazolyl)propyl acrylate) (CPA) brushes showed a better turn-on voltage of 5 V compared to 20 V on native ITO on an ITO/CPA/Alq_3/LiF/Al.[49] The devices were further optimized by UV irradiation and ion-assisted deposition with $I-V$ and $L-V$ reaching 100 mA/cm^2 (7.5 V) and 1000 Cd/m^2 (10.0 V). Comparative device performance on electropolymerized and cross-linked PVK brush films can also be investigated in the future to compare with devices prepared on non-cross-linked substrates. We have previously reported the use of electropolymerized and cross-linked PVK as a hole-transport material on ITO in which the HOMO was determined to be variable from 5.1 to 5.4 eV.[31] The $I-V$ and $L-V$ showed variable behavior depending on the doping level of the electropolymerized PVK film. Doping increases hole injection through the PVK film but also results in a greater electron injection from the polyfluorene layer which tends to decrease luminance. Further studies will be made to elucidate the role of doping for these films with respect to $I-V$ and $L-V$ performance.

Nevertheless, the ability to use spin-casting to deposit a polymeric electroluminescent active layer, e.g. polyfluorene, onto a spin-coated PVK hole transport layer has previously been impractical due to mutual dissolution. Through the use of the SIP

technique we were able to overcome this obstacle and produce a robust hole-transport layer of PVK with good PLED performance.

Conclusions

The SIP grafting technique was successfully utilized to functionalize the conducting transparent electrode ITO with the hole-transporting PVK brushes. This resulted in the formation of homogeneous films with smooth domains and features enabling the morphological passivation of ITO and at the same time improve the hole-transport properties of the transparent electrode. The PVK brush in turn can be electrochemically cross-linked, by cyclic voltammetry measurements, to form a conjugated polymer network film. The covalent linkage of the PVK allowed for a direct electroluminescent PLED device preparation in which the EL polymer layer can be simply solution-cast onto the modified ITO irrespective of solubility. In the future, this should open up a variety of other wet processing methods for device preparation independent of adding a preliminary hole-transport layer on the modified ITO. Further optimization can be done by correlating thickness, interfacial structure, composition, and solvent treatment of the hole-transporting brush.

Experimental Section

Materials. THF was freshly distilled over a sodium benzophenone ketal and collected immediately prior to use. All other reagents were analytical grade quality, purchased commercially from Aldrich Chemical Co., and used without further purification.

Analytical Techniques. ^{1}H and ^{13}C NMR spectra were recorded on a General Electric QE 300 spectrometer (300 MHz). UV−vis measurements were taken on an Agilent technologies 8453 spectrometer. The SEC analysis was performed using a Viscotek 270 quad detector equipped with VE3210 UV/vis detector and VE3580 RI detector. FTIR measurements were done using a Digilab FTS 7000 step scan spectrometer. Atomic force microscopy (AFM) images were obtained in MAC mode with a PicoPlus PicoScan 1500 (Agilent Technologies formerly Molecular Imaging, Inc.) at 25 °C and 50% humidity. A Molecular Imaging type II MAC lever tip with a spring constant of 2.8 N/m and a resonance frequency of 75 kHz was used at a scan rate of 10 000 nm/s. All image processing was performed with SPIP evaluation software (Scanning Probe Image Processor, Image Metrology). Contact angle goniometry was conducted using a KSV CAM 200 instrument (KSV Ltd.) using the bubble drop method with water. X-ray photoelectron spectroscopy (XPS) was carried out on a Physical Electronics 5700 instrument with photoelectrons generated by the nonmonochromatic Al Kα irradiation (1486.6 eV). Photoelectrons were collected at a takeoff angle of 45° using a hemispherical analyzer operated in the fixed retard ratio mode with an energy resolution setting of 11.75 eV. The binding energy scale was calibrated prior to analysis using the Cu $2p_{3/2}$ and Ag $3d_{5/2}$ lines. Charge neutralization was ensured through cobombardment of the irradiated area with an electron beam and the use of the nonmonochromated Al Kα source, placing the C 1s peak at a binding energy of 284.6 (0.2) eV.

Synthesis of (*E*)-2-(Chlorodimethylsilyl)ethyl-4-((5-butoxy-2-cyano-5-oxopentan-2-yl)diazenyl)-4-cyanopentanoate (AIBNSiCl) (Scheme 1). Under an inert atmosphere, 3.0 g (11 mmol) of 4,4′-azobis(4-cyanovaleric acid) and 79 mg of (dimethylamino)pyridine (DMAP) were dissolved in 0.7 g of butanol and 25 mL of tetrahydrofuran (THF). The solution was cooled to 0 °C, and then 2.2 g (11 mmol) of dicylcohexylcarbodiimide (DCC) in 50 mL of THF was slowly added dropwise to the dissolved mixture with vigorous stirring. The reaction mixture was allowed to react at 0 °C for 5 min and then allowed to warm to room temperature and continue reaction for 3 h. The urea was filtered, and the filtrate was poured into water, extracted with methylene chloride, washed by saturated sodium bicarbonate, and dried over magnesium sulfate. After the solvent was evaporated, the residue was solidified by pouring into cold hexanes. The solid was collected, dried, and used for the next step without further purifications. ^{1}H NMR (in $CDCl_3$, δ in ppm): 4.11 (2H,t, 6.6 Hz), 2.47 (8H, m), 1.74 (3H, s), 1.68 (3H, s), 1.62 (2H, m), 1.37 (2H, m), 0.94 (3H, t, 7.3 Hz). The solid was combined with 1 equiv of allyl alcohol, and the same DCC/DMAP reaction was carried out again. ^{1}H NMR (in $CDCl_3$, δ in ppm): 5.88 (1H, m), 5.25 (2H, dd, 7.3 Hz), 4.6 (2H, d, 6.1 Hz), 4.11 (2H, t, 6.6 Hz), 2.47 (8H, m), 1.74 (3H, s), 1.68 (3H, s), 1.62 (2H, m), 1.37 (2H, m), 0.94 (3H, t, 7.7 Hz). 7.5 g (20 mmol) of the crude product and 1.0 mg of hydrogen hexachloroplatinate(IV) hydrate were dissolved in 15 mL of THF. Under an inert atmosphere, 3.3 mL of dimethylchlorosilane in 25 mL of THF was added. The solution was stirred at 0 °C and allowed to warm to room temperature. Solvent and excess dimethylchlorosilane were removed on a rotary evaporator at 35 °C, and the residue was collected. The residue was dried under high vacuum using a Schlenk line, yielding a slightly yellowish oil that was stored under nitrogen to protect from moisture and used without any further purification. Any bischlorosilane impurity will occupy more space on the substrate but should not affect brush growth. ^{1}H NMR (in $CDCl_3$, δ in ppm): 4.11 (4H, m), 2.47 (8H, m), 1.74 (3H, s), 1.68 (3H, s), 1.62 (2H,m), 1.37 (2H, m), 0.94 (3H, t, 7.3 Hz), 0.8 (2H, m), and 0.4 (6H, s). Decomposition with thermogravimetric analysis (TGA) was observed at 120 °C, corresponding to the activation and evolution of N_2 gas from the material resulting in a 6.34% mass (calculated, 6.14% at 28 g/mol N_2 and 456.2 g/mol AIBNSiCl.)

Substrate Modification. Preparation of the AIBNSiCl SAM initiator were carried out by the addition of 0.5 wt % (m/v) of AIBNSiCl in toluene to clean silicon wafers or ITO in a slide staining jar. 1 ml of pyridine was added to catalyze the surface condensation reaction and also to act as an acid scavenger. The substrates were left in the solution for 12−24 h to ensure complete SAM formation of AIBNSiCl. The slides were then rinsed and sonicated in methanol to remove the pyridinium hydrochloride salt that was formed in the reaction. The substrates were then stored in isopropanol in a dark cabinet to ensure no decomposition and protection from dust.

Polymerization. The functionalized substrates were placed vertically in a Teflon holder to separate the slides. The slides were then placed in a Schlenk flask with a small magnetic stirring bar, 2.0 g of 9-vinylcarbazole, and 25 mL of freshly distilled toluene. Three to four freeze−pump−thaw cycles were performed on the reaction mixture to remove all dissolved gases. The Schlenk flask was then put under positive pressure of nitrogen and placed in a constant temperature bath at 70 °C. Thermal degradation of the nitrile bond produces a bound and an unbound radical that rapidly undergoes addition to the vinyl bond of the 9-vinylcarbazole. The chain reaction is extremely prolific and is complete in ∼1 s. The longer the reaction is kept at elevated temperatures, the thicker the brush will appear; this is not due to a longer polymer chain but due to a higher density of polymer chains extending from the surface. The solution was allowed to stir for 6−24 h, after which the flask was removed from the bath and allowed to cool to room temperature. The solution was added dropwise to a large excess of methanol to precipitate the free polymer formed from the unbound radical and saved for GPC measurements. The Teflon holder and slides were placed in a Soxhlet extractor for continuous extraction with THF for 24 h to remove all unbound polymer from the substrate surfaces. The slides were placed in a slide mailer and stored in a vacuum desiccator until needed.

Electrochemistry. All electrochemical modifications were performed using a Partsat 2263 and Powersuite software (Princeton Applied Research, Inc.) A three-electrode cell system was used with counter, reference, and working electrodes. The counter electrode was a Pt plate electrode, the reference electrode was a freshly prepared Ag/AgCl nonaqueous electrode (NHE for HOMO−LUMO determination), and the working electrode was the ITO-coated glass substrate. TBAH or TBAP (perchlorate) was used as electrolytes.

Device Assembly. ITO-coated glass with resistance of ∼0.3 ohm was purchased from SPI Supplies in 30 cm^2 sheets. The substrates were cut into 1 $in.^2$ pieces then washed with detergent (Alconox) in Milli-Q quality water to remove any dust and glass particulates from the cutting procedure. The slides were then sonicated for 15

min in a series of solvents, deionized water, isopropanol, hexane, and toluene; the substrates were then dried under a stream of nitrogen. Two parallel strips of Scotch brand clear tape were placed on the ITO surface to mask against HCl acid etching; the substrates were placed in a 1:1 H_2O:HCl solution for 20 min. After etching, the substrates were sonicated in H_2O, acetone, and isopropanol for 15 min each, after which the tape was removed and the substrates were cleaned again. The substrates were dried with nitrogen and placed into the plasma cleaner for a period of 2 min and then were treated with the aforementioned substrate modification technique. Polymerization was carried out for a period of 12 h to produce the hole-transport layer of the sandwich device. The substrates were cleaned by Soxhlet extraction for 24 h to ensure the complete removal of any physically adsorbed PVK. The substrates were taken from the Soxhlet apparatus and immediately transferred to the spin-coater, and a solution of the electroluminescent polymer (P14-FL)[37] (1.9 mg/mL) in freshly distilled toluene was cast at 1000 rpm, giving a ca. 90 nm electroluminescent layer. The substrate was transferred to a vacuum oven for a period of 1 h at 25 °C, after which the substrate was moved to a thermal evaporator (Edwards E306) where aluminum deposition was carried out at below 10^{-6} Torr through a mask making perpendicular electrodes to the underlying ITO electrodes. The samples were allowed to cool in the evaporator for a period of 1 h before removal and immediate coverage of the working device area with an epoxy resin to limit oxygen permeation of the device during testing. PLED testing was done using a Keithley 236 source meter unit, a Hamamatsu photonics photomultiplier, and an in-house written Laboratory-View program. Current−voltage−luminescence data were collected from 0 to 10 V at steps of 0.10 V. Conversion of luminescence data to Cd/m^2 from photon counts is based on calibration with previous $L-V$ measurements using an ITO/PVK/polyfluorene/Al hole-only PLED device that has been previously reported.[31]

Acknowledgment. Support for this work from NSF CHE-03-04807, DMR-03-15565, DMR-0602896, and ACS-PRF-45853-AC7 Grant, and the Alliance for Nanohealth of Texas is gratefully acknowledged. The authors also thank Agilent Technologies Inc., Viscotek Inc., Optrel GmBH, and KSV Instruments Inc. for help with technical assistance on the AFM, ellipsometer, and WCA measurements.

Supporting Information Available: DSC and TGA data, atomic force microscopy images of ITO and electropolymerized brush films, detailed procedures, and high-resolution XPS scans with curve fitting. This material is available free of charge via the Internet at http://pubs.acs.org.

References and Notes

(1) Skotheim, T. A.; Reynolds, J. R. *Handbook of Conducting Polymers*, 3rd ed.; CRC Press: Boca Raton, FL, 2007.
(2) Shirota, Y.; Kakuta, T.; Kanega, H.; Mikawa, H. *Chem. Commun.* **1985**, 1201–1202.
(3) (a) Burrows, P. E.; Forrest, S. R.; Sibley, S. P.; Thompson, M. E. *Appl. Phys. Lett.* **1996**, *69*, 2959–2961. (b) Mori, T.; Obata, K.; Imaizumi, K.; Mizutani, T. *Appl. Phys. Lett.* **1996**, *69*, 3309–3311.
(4) Michelotti, F.; Borghese, F.; Bertolotti, M.; Cianci, E.; Foglietti, V. *Synth. Met.* **2000**, *111−112*−108.
(5) Ling, Q. D.; Lim, S. L.; Song, Y.; Zhu, C. X.; Chan, D. S. H.; Kang, E. T.; Neoh, K. G. *Langmuir* **2007**, *23*, 312–319.
(6) Papez, V.; Josowicz, M. *J. Electroanal. Chem.* **1994**, *365*, 139–150.
(7) Tamada, M.; Omichi, H.; Okui, N. *Thin Solid Films* **1995**, *268*, 18–21.
(8) Kido, J.; Shionoya, H.; Nagai, K. *Appl. Phys. Lett.* **1995**, *67*, 2281–2283.
(9) Choudhury, K. R.; Samoc, M.; Patra, A.; Prasad, P. N. *J. Phys. Chem. B* **2004**, *108*, 1556–1562.
(10) Lee, C. L.; Das, R. R.; Kim, J. J. *Chem. Mater.* **2004**, *16*, 4642–4646.
(11) van Dijken, A.; Bastiaansen, J. J. A. M.; Kiggen, N. M. M.; Langeveld, B. M. W.; Rothe, C.; Monkman, A.; Bach, I.; Stossel, P.; Brunner, K. *J. Am. Chem. Soc.* **2004**, *126*, 7718–7727.
(12) (a) Tomova, R.; Petrova, P.; Stoycheva-Topalova, R. *J. Optoelectron. Adv. Mater.* **2007**, *9*, 501–504. (b) Berkovich, E.; Klein, J.; Sheradsky, T.; Silcoff, E.; Ranjit, K.; Willner, I.; Nakhmanovich, G.; Gorelik, V.; Eichen, Y. *Synth. Met.* **1999**, *107*, 85–91. (c) Qui, Y.; Duan, L.; Hu, X.; Zhang, D.; Zheng, M.; Bai, F. *Synth. Met.* **2001**, *123*, 39–42. (d) Zhang, C.; vonseggern, H.; Pakbaz, K.; Kraabel, B.; Schmidt, H.; Heeger, A. *Synth. Met.* **1994**, *62*, 35–40.
(13) Davenas, J.; Besbes, S.; Ouada, H. B.; Majdoub, M. *Mater. Sci. Eng., C* **2002**, *21*, 259–264.
(14) Kawde, R. B.; Laxmeshwar, N. B.; Santhanam, K. S. V. *Sens. Actuators, A* **1995**, *23*, 35–39.
(15) Kawde, R. B.; Santhanam, K. S. V. *Bioelectrochemistry* **1995**, *38*, 405–409.
(16) Skompska, M.; Hillman, A. R. *J. Electroanal. Chem.* **1997**, *433*, 127–134.
(17) Borjas, R.; Buttry, D. A. *J. Electroanal. Chem.* **1990**, *280*, 73–90.
(18) Romero, D. B.; Nuesch, F.; Benazzi, T.; Ades, D.; Siove, A.; Zuppiroli, L. *Adv. Mater.* **1997**, *9*, 1158.
(19) Desbenemonvernay, A.; Dubois, J. E.; Lacaze, P. C. *J. Electroanal. Chem.* **1985**, *189*, 51–63.
(20) Skompska, M.; Peter, L. M. *J. Electroanal. Chem.* **1995**, *383*, 43–52.
(21) Sebastian, R. M.; Caminade, A. M.; Majoral, J. P.; Levillain, E.; Huchet, L.; Roncali, J. *Chem. Commun.* **2000**, 507–508.
(22) Deng, S. X.; Advincula, R. C. *Chem. Mater.* **2002**, *14*, 4073–4080.
(23) (a) Taranekar, P.; Baba, A.; Fulghum, T. M.; Advincula, R. *Macromolecules* **2005**, *38*, 3679–3687. (b) Taranekar, P.; Fulghum, T.; Baba, A.; Patton, D.; Advincula, R. *Langmuir* **2007**, *23*, 908–917.
(24) Taranekar, P.; Fan, X.; Advincula, R. *Langmuir* **2002**, *18*, 7943–7952.
(25) Inaoka, S.; Roitman, D. B.; Advincula, R. C. *Chem. Mater.* **2005**, *17*, 6781–6789.
(26) Park, M. K.; Xia, C.; Advincula, R. C.; Schutz, P.; Caruso, F. *Langmuir* **2001**, *17*, 7670–7674.
(27) Jang, S. Y.; Sotzing, G. A.; Marquez, M. *Macromolecules* **2002**, *35*, 7293–7300.
(28) Xia, C.; Fan, X.; Park, M. K.; Advincula, R. C. *Langmuir* **2001**, *17*, 7893–7898.
(29) Fulghum, T.; Karim, S. M. A.; Baba, A.; Taranekar, P.; Nakai, T.; Masuda, T.; Advincula, R. C. *Macromolecules* **2006**, *39*, 1467–1473.
(30) Xia, C.; Advincula, R. C.; Baba, A.; Knoll, W. *Chem. Mater.* **2004**, *16*, 2852–2856.
(31) Baba, A.; Onishi, K.; Knoll, W.; Advincula, R. *J. Phys. Chem. B* **2004**, *108*, 18949–18955.
(32) Jegadesan, S.; Sindhu, S.; Advincula, R. C.; Valiyaveettil, S. *Langmuir* **2006**, *22*, 780–786.
(33) Jegadesan, S.; Taranekar, P.; Sindhu, S.; Advincula, R. C.; Valiyaveettil, S. *Langmuir* **2006**, *22*, 3807–3811.
(34) (a) Ejaz, M.; Yamamoto, S.; Ohno, K.; Tsujii, Y.; Fukuda, T. *Macromolecules* **1998**, *31*, 5934–5936. (b) Husseman, M.; Malmstrom, E. E.; McNamara, M.; Mate, M.; Mecerreyes, D.; Benoit, D. G.; Hedrick, J. L.; Mansky, P.; Huang, E.; Russell, T. P.; Hawker, C. J. *Macromolecules* **1999**, *32*, 1424–1431. (c) Kamigaito, M.; Ando, T.; Sawamoto, M. *Chem. Rev.* **2001**, *101*, 3689–3745.
(35) Advincula, R.; Ruhe, J.; Brittain, W.; Caster, K. E. *Polymer Brushes: On the Way to Tailor-Made Surfaces*; 1st ed.; Wiley-VCH: New York, 2004.
(36) Jhaveri, S.; Carter, K. *Langmuir* **2007**, *23*, 8288–8290.
(37) Taranekar, P.; Abdulbaki, M.; Krishnamoorti, R.; Phanichphant, S.; Waenkaew, P.; Patton, D.; Fulghum, T.; Advincula, R. *Macromolecules* **2006**, *39*, 3848–3854.
(38) Zhan, X.; Wang, S.; Liu, Y.; Wu, X.; Zhu, D. *Chem. Mater.* **2003**, *15*, 1963–1969.
(39) (a) Snaith, H. J.; Whiting, G. L.; Sun, B.; Greenham, N. C.; Huck, W. T. S.; Friend, R. H. *Nano Lett.* **2005**, *5*, 1653–1657. (b) Whiting, G. L.; Snaith, H. J.; Khodabakhsh, S.; Andreasen, J. W.; Breiby, D. W.; Nielsen, M. M.; Greenham, N. C.; Friend, R. H.; Huck, W. T. S. *Nano Lett.* **2006**, *6*, 573–578.
(40) Katsuki, K.; Bekku, H.; Kawakami, A.; Locklin, J.; Patton, D.; Tanaka, K.; Advincula, R.; Usui, H. *Jpn. J. Appl. Phys.* **2005**, *44*, 504–508.
(41) Prucker, O.; Rühe, J. *Macromolecules* **1998**, *31*, 592–601.
(42) Fulghum, T. M.; Patton, D. L.; Advincula, R. C. *Langmuir* **2006**, *22*, 8397–8402.
(43) (a) Prucker, O.; Rühe, J. *Langmuir* **1998**, *14*, 6893–6898. (b) Limpoco, F.; Advincula, R.; Perry, S. *Langmuir* **2007**, *23*, 12196–12201.
(44) Kaholek, M.; Lee, W.-K.; Ahn, S.-J.; Ma, H.; Caster, K. C.; LaMattina, B.; Zauscher, S. *Chem. Mater.* **2004**, *16*, 3688–3696.
(45) Taranekar, P.; Fulghum, T.; Baba, A.; Patton, D.; Advincula, R. *Langmuir* **2007**, *23*, 908–917.
(46) Syed Abthagir, P.; Saraswathi, R. *Org. Electron.* **2004**, *5*, 299–308.
(47) Hayashida, S.; Sukegawa, K.; Niwa, O. *Synth. Met.* **1990**, *35*, 253–261.
(48) Abe, S. Y.; Bemede, J. C.; Delvalle, M. A.; Tregouet, Y.; Ragot, F.; Diaz, F. R.; Lefrant, S. *Synth. Met.* **2002**, *126*, 1–6.
(49) Kawakami, A.; Katsuki, K.; Advincula, R.; Tanaka, K.; Ogino, K.; Usui, H. *Jpn. J. Appl. Phys.* **2008**, *47*, 3156–3161.

MA800341A